ground water

Localized Thermal Anomalies in Haloclines of Coastal Yucatan Sinkholes

by Ronald K. Stoessell[1], James G. Coke[2], and Dale H. Easley[1]

Abstract

A temperature spike is reported in the haloclines of three Yucatan sinkholes along a 1 km NW-SE transect from 5 to 4 km inland from the Caribbean coast. The temperature spike decreases in magnitude from ~ 3.5°C to 0.2°C, approaching the coast. The anomaly does not vary diurnally and does not extend down into the underlying sea water. These conditions are inconsistent with explanations such as radiation absorption within the halocline, in situ microbially mediated sulfate reduction within the halocline and the underlying sea water, and sulfide oxidation by photosynthetic purple and green bacteria within the halocline.

One explanation consistent with the shape and halocline location of the temperature spike involves a localized sea water convection cell operating near the coast. Cold sea water from the Caribbean Sea enters the coastal limestone at depths of a few hundred meters and heats up because of the geothermal gradient, buoyantly rising in vertical fractures within the unconfined aquifer. Blocked by the less dense fresh water, the movement stops in the halocline where the warm sea water mixes with brackish water. The convection cycle would be completed by the coastward movement of cooling brackish water. The observed temperature anomalies could possibly be snapshots of this warm layer moving coastward.

Introduction

The northeastern coastal Yucatan Peninsula, adjacent to the Caribbean Sea, is a region of karst topography (Back and Hanshaw 1970) with numerous sinkholes and some of the longest subaquatic cave systems discovered (Coke and Young 1989; Coke et al. 1990). The area is underlain by an unconfined Pleistocene limestone aquifer (Back and Hanshaw 1970), in which high-magnesium calcite has dissolved or been replaced by low-magnesium calcite, and dissolution of aragonite is an on-going process, driven by CO_2 absorption and the mixing of fresh water and sea water in the halocline (Hanshaw and Back 1980; Ward and Halley 1985; Ford 1985; Back et al. 1986; Stoessell et al. 1989). Mixing-zone dolomitization has occurred within the saline portion of the coastal Pleistocene halocline (Ward and Halley 1985). Saline dolomitization of limestone was explained by the high alkalinity and CO_2 partial pressure of the coastal Yucatan fresh water endmember (Stoessell et al. 1989). The interior and coastal sinkholes typically show the effects of sulfate reduction and sulfide oxidation where the present halocline lies above the sinkhole floor (Socki 1984; Stoessell et al. 1993), and magnesium deficiencies in the underlying sea water of some of the sinkholes imply limestone dolomitization is presently occurring (Marcella 1994).

The thin fresh water lens (generally less than 70 m thick in the northern Yucatan Peninsula) is characterized by low hydraulic heads (Back and Hanshaw 1970; Moore et al. 1992) and is thinner than predicted by either the static Ghyben-Herzberg model or the nonstatic fresh water model of Hubbert (1940) (Moore et al. 1992; Beddows 1999). The halocline is typically narrow and sharp (Moore et al. 1992) and has been reproduced by modeling its formation as a diffusion boundary between layers of sea water and fresh water (Stoessell 1995). Tidal effects are negligible in the nonfracture pore porosity a few kilometers inland (Moore et al. 1993) but become significant in fractures connected directly to the coast (Beddows 1999). The nonstatic nature of the sea water was shown by velocity measurements (discussed later) by Moore et al. (1992) and Soteres (2000) in the porous medium regime and in the fracture regime.

This paper resulted from an examination of temperature data taken in deep coastal Yucatan sinkholes over the last 12 years. The depth versus temperature profiles showed unex-

---

[1] Department of Geology and Geophysics, University of New Orleans, New Orleans, LA 70148; rstoesse@uno.edu and deasley@uno.edu

[2] P.O. Box 8663,The Woodlands, TX 77387; chac@lcc.net

Received August 2001, accepted April 2002.

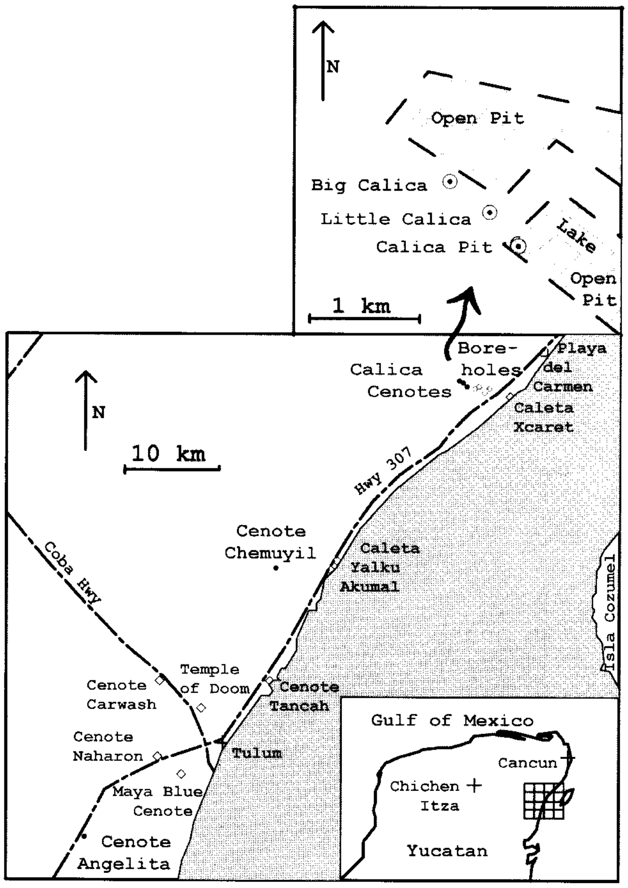

Figure 1. Location map of sinkholes (cenotes), sketched from road maps with GPS data.

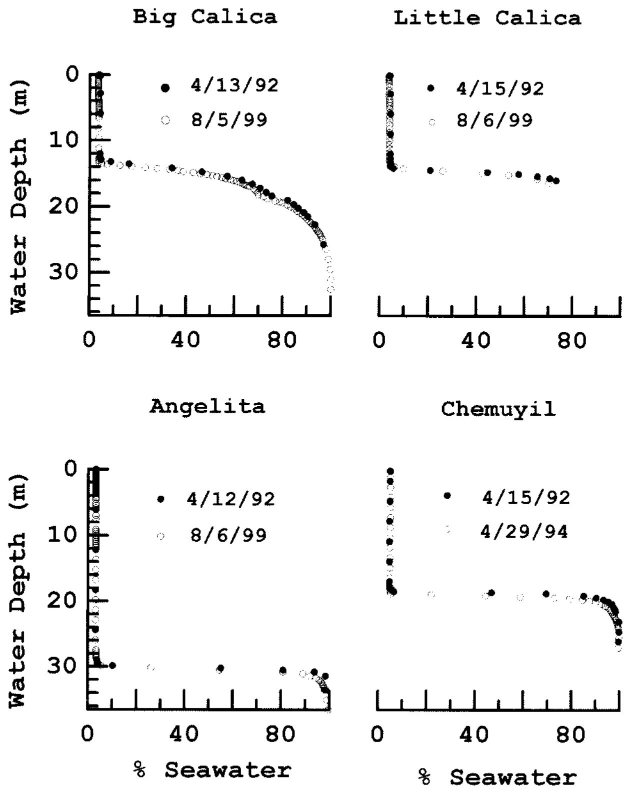

Figure 2. Historical records of water depth versus percentage of sea water in coastal Yucatan sinkholes.

pected temperature spikes in the haloclines of two adjacent sinkholes on Calica property near Playa del Carmen (Figure 1). An additional temperature anomaly was measured in 2001 in a nearby sinkhole exposed by surface mining operations. The data are examined and various explanations are considered to explain the origin of the anomalies.

We were not able to find published papers where heat anomalies in coastal sinkholes have been reported within and below the halocline. Explanations such as radiation absorption and exothermic chemical reactions are evaluated here because the authors have previously documented sulfur redox reactions occurring in these sinkholes (Stoessell et al. 1993) and observed reddish, opaque water in sinkholes within and below their haloclines.

Sea water convection under the fresh water lens in coastal limestones is not a new idea but evidence for it has been generally lacking or indirect. However, convection is consistent with the flow measurements of Moore et al. (1992) and Soteres (2000) in which sea water just below the halocline was shown to be moving coastward. Cooper (1959) predicted small-scale convection in coastal regions because of the daily oceanic tides. Sanford and Konikow (1989a, 1989b) showed underlying sea water circulating through the mixing zone in a numerical model of coastal carbonate aquifers, forced by their model's boundary conditions. Whitaker and Smart (1990) postulated coastward movement of sea water under the Great Bahama Bank. They suggested the movement is driven either by density differences caused by saline reflux of brines with subsequent mixing with sea water (Simms 1984) and/or hydraulic head differences across the carbonate platform generated by the Florida Current and by Atlantic storm systems.

Kohout (1965, 1967) and Fanning et al. (1981) presented evidence for deep sea water convection under the West Florida continental shelf. The discharge of thermal springs on the Gulf of Mexico sea floor near the coast was hypothesized to be caused by the penetration of the permeable Florida aquifer by cold sea water, which heats up and buoyantly rises to emerge as warm springs near the west coast of southern Florida. The sea water has been altered presumably by limestone dolomitization, producing an excess of aqueous calcium and a deficiency of magnesium (Fanning et al. 1981).

Thermally driven sea water convection has also been deduced to occur under Pacific atolls in which the heat source is the residual heat from underlying seamounts (Swartz 1958). Saller (1984) postulated thermally driven convection could have brought in cold ocean water up through Enewetak atoll, providing the fluid for observed subsurface dolomitization. Aharon et al. (1987) used isotopes and chemical gradients in dolomites to postulate that thermal convection occurs under Niue atoll in the South Pacific.

The literature contains no reports of igneous intrusions that could affect the thermal regime under the Caribbean coast of the Yucatan. The geothermal gradient is the major source of heat. This paper provides thermal evidence for thermally driven sea water convection within a coastal carbonate platform.

Historical Data Record in Several Coastal Yucatan Sinkholes

Locations of several deep vertical sinkholes (known locally as "cenotes") along the northeastern coast of the Yucatan Peninsula are shown in Figure 1. Profiles of water depth versus percentage of sea water (Figure 2) and water depth versus temperature (Figure 3) are shown for Big Calica Cenote, Little Calica Cenote, Cenote Angelita, and Cenote Chemuyil. The term sea water is used rather than saline ground water because of its chemical composition (Stoessell et al. 1989, 1993). These cenotes are classic circular sinkholes with vertical walls, varying in diameter from approximately 20 m at Angelita, to 35 m at Little Calica and Chemuyil and 45 m at Big Calica. Surface elevations are less than 15 m at Big Calica, Little Calica, and Chemuyil and 3 m at Angelita, and the water table is less than a meter above mean sea level (Moore et al. 1992). The sinkhole depths extend below the present fresh water lens, reflecting their formation during Pleistocene ice ages when sea level was lower (Stoessell 1994a).

All of these sinkholes have anaerobic haloclines and anaerobic underlying sea water, as evidenced by the occurrence of sulfide, sulfate depletion, and lower than expected pH values. These are reported in water samples from Big Calica, Little Calica, and Angelita by Chen (1991), Stoessell et al. (1993), and Marcella (1994). Unpublished data by Stoessell (available upon request) has verified their occurrence in Chemuyil. Falling organic matter accumulates in the bottom of the sinkholes where its decay makes the sea water anaerobic. Because the halocline is above the sinkhole bottom, sea water provides sulfate for sulfate reduction in the presence of the decaying organic matter. Aqueous sulfide accumulates in the anaerobic halocline and underlying sea water. Some of the sulfide is oxidized back to sulfate by photosynthetic purple and green bacteria in the anaerobic water of the halocline and by aerobic Thiobacillus sulfide-oxidizing bacteria in the overlying fresh water (Stoessell et al. 1993).

Conductivity and temperature data were taken with a modified YSI 3000 probe (YSI Inc., Yellow Springs, Ohio) in April 1992 and August 1999 for the first three sinkholes and in April 1992 and April 1994 in Chemuyil, and are representative of available historical data for these sinkholes. The two data sets coincide closely for each sinkhole in Figure 2, showing the general stability with time of water depth versus salinity profiles. The haloclines are vertically narrow and nearly linear (water depth versus percentage of sea water) in Angelita and Chemuyil (Figure 2).

The shape and width of the halocline in Angelita has been successfully modeled by assuming diffusion between two immiscible fluids, an upper fresh water and underlying sea water, both moving at the same velocity toward the coast (Stoessell 1995). This simplistic model apparently worked because of the dampening effect on transverse dispersion caused by the mechanical stability of the less dense fresh water overlying the sea water. The nonstatic nature of the underlying sea water was recently confirmed in Angelita by Soteres (2000) who used fluorescent dye to measure velocities of ~0.3 cm/sec in the same direction above and below the halocline in Angelita. Moore et al. (1992) measured velocities of fresh water and sea water of 0.002 and 0.008 cm/sec, respectively, by point dilution in a Calica borehole. Her lower velocities are attributed to the lower permeability in the pore-dominated rock; however, her sea water velocity was measured near a fracture that cut the borehole.

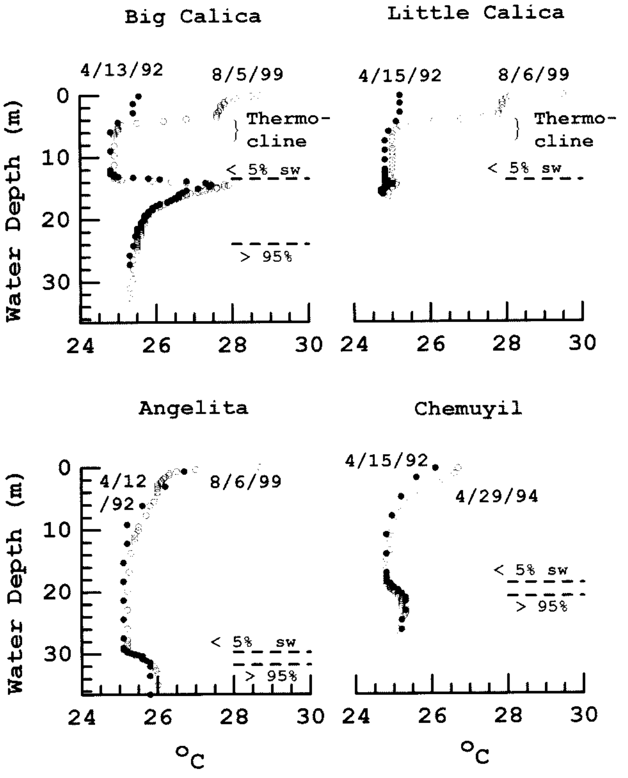

Figure 3. Historical records of water depth versus temperature in coastal Yucaton sinkholes.

The halocline in Big Calica Cenote (Figure 2) has a much greater vertical width and is more nonlinear in profiles of water depth versus percentage of sea water than in Angelita and Chemuyil. Little Calica bottoms out before the bottom of the halocline is reached, obscuring the profile of the complete halocline. The profile of the halocline in Big Calica has been suggested as caused by the intersection of fractures producing mixing of different ground waters (Stoessell 1995).

Profiles of water depth versus temperature, corresponding to the profiles of percentage of sea water in Figure 2, are shown in Figure 3. Sharp changes in temperature with depth occur at the halocline/fresh water interface, illustrating that temperature changes can often be used to delineate the interface, as suggested by Taniguchi (2000). Note the overlap in the temperature profiles in the vicinity of the haloclines, showing a stable thermal regime with time. The effects of surface heating are also shown in the profiles, extending to depths of nearly 10 m in Angelita and Chemuyil and 5 m in the Calica sinkholes. The sea water under the halocline is ~1.0°C warmer than the overlying fresh water in Angelita and Chemuyil and ~0.5°C warmer in Big Calica. The bottom temperature (70% sea water) of Little Calica is within 0.1°C of the overlying fresh water.

Nearly linear profiles of depth versus temperature occur in Angelita and Chemuyil across their narrow halo-

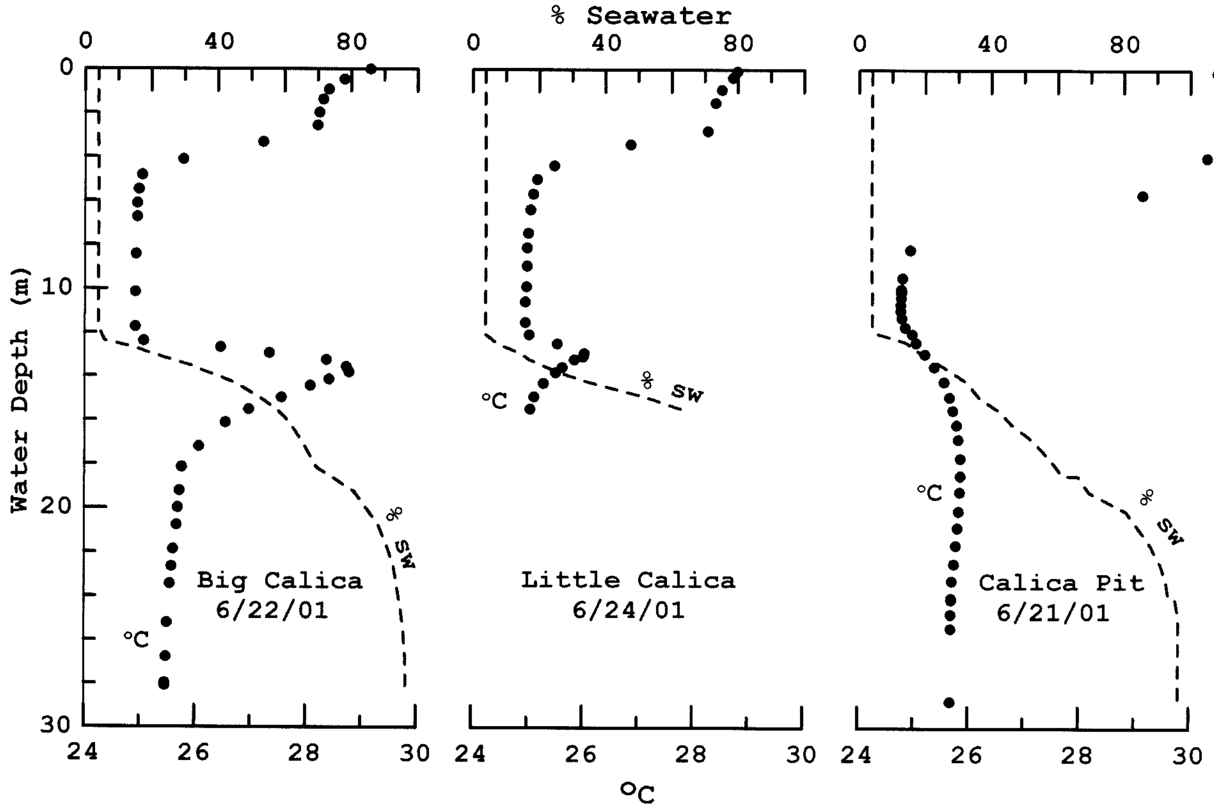

Figure 4. In 2001, temperature and percentage of sea water versus water depth in three Calica sinkholes, which lie along a 1 km coastward traverse (to the right), and each has a thermal anomaly in the halocline.

clines, suggesting heat conduction upward from the underlying sea water is controlling the temperature profile. There is an indication in Chemuyil of a 0.1°C decrease in sea water temperature below the halocline.

A temperature spike, ~2.6°C above the underlying sea water temperature and 3.0°C above the overlying fresh water temperature, was observed within the halocline of Big Calica. A temperature spike shows up in the four sets of data taken in Big Calica, beginning with the earliest data set in 1992. The profile of the temperature spike is nearly linear on its upper side, ~1.2 m wide, and nonlinear on its lower side, ~15 m wide. A much reduced temperature spike, ~0.2°C, is shown within the halocline in Little Calica. Six data sets were taken in the 1990s from Little Calica and the small temperature spike shows up in all of them, beginning with the earliest data set in 1990.

Several Calica boreholes are located between Little Calica and Highway 307, as shown in Figure 1. Their water depth versus percentage of sea water profiles have been reported elsewhere (Chen 1991; Moore et al. 1992; Stoessell et al. 1993). These profiles are narrow and linear in the halocline, unlike that in Big Calica. Halocline temperature spikes are not present in unpublished temperature data (available by request). Apparently, ground water passing through the sinkholes is primarily flowing through fractures, bypassing the less-permeable pore system in the surrounding limestone.

Recent Depth Profiles: Percentage of Sea Water and Temperature in Calica Sinkholes

In June 2001 the Calica sinkholes were revisited with a YSI 6600 sonde (YSI Inc., Yellow Springs, Ohio) on a 75 m cable with a 650 MDS (multiparameter display system, YSI Inc.) data logger to make detailed temperature profiles. The precise locations of the two sinkholes and at Calica Pit, a sinkhole recently exposed by surface mining, were mapped by GPS (global positioning system) and are shown in Figure 1. The three sites lie along a 0.9 km transect trending northwest-southeast from Big Calica to Little Calica to the Calica Pit and are separated, respectively, by 0.5 and 0.4 km. From Calica Pit, a 4.3 km continuation of the transect reaches the coast (off the enlarged Calica area in Figure 1).

Big Calica and Little Calica are separated by 100 to 200 m of jungle from the open-pit mine (Figure 1). Calica Pit is a 50 m deep, vertical hole at the southwest corner of the mine and is at one end of an artificial lake created by dredging in the fresh water lens. Dredging was ongoing during the site visit, several hundred meters from the pit, and was a source of mixing in the fresh water lens in the lake. The pit's location precludes jungle vegetation from falling into the halocline and underlying sea water to drive sulfate reduction.

Depth versus temperature and salinity profiles in 2001 are overlapped at each of the three sites in Figure 4. The sites were on the southwest side of Big Calica and Little Calica and over the center of Calica Pit. Depths have been corrected for changes in density above the YSI 6600 sonde, which computes depth without keeping track of these den-

Table 1
Hypotheses for Explaining the Temperature Spikes

Possible Explanation	Consistent Observations	Inconsistent Observations
Absorption of light radiation in halocline	1. Temperature spike is located near the top of halocline (Figures 3, 4, and 7).	1. Lack of temperature spike decrease at night (Figure 5). 2. Spike is not present in all coastal sinkholes (Figure 3).
Photosynthesis oxidation of sulfide to sulfate by anaerobic purple and green bacteria	1. The reddish color of these bacteria have been observed in the halocline of all coastal sinkholes which show evidence of sulfate reducation (water samples by Chen 1991; Stoessell et al. 1993; Marcella 1994; Stoessell 1992, 1994b).	1. Lack of temperature spike decrease at night (Figure 5). 2. Spike is not present in all coastal sinkholes (Figure 3). 3. Spike is present in Calica Pit, which does not have anaerobic water (Figure 4).
Anaerobic bacteria sulfate reduction	1. Most coastal sinkholes show evidence of sulfate reduction if halocline lies above bottom (water samples by Chen 1991; Stoessell et al. 1993; Marcella 1994; Stoessell 1992, 1994b).	1. Temperature spike does not extend into underlying sea water in coastal cenotes (Figures 3 and 4). 2. Spike is not present in all coastal sinkholes, which have sulfate reduction (Figure 3). 3. Spike is present in Calica Pit, which does not have anaerobic water (Figure 4).
Return arm of geothermal sea water convection cell	1. Sea water under the halocline is moving coastward (Moore et al. 1992; Stoessell 1995; Stoessell 2000). 2. The temperature spike is only in the halocline (Figures 3 and 4). 3. The temperature gradient is linear above spike and concave below spike (Figure 4). 4. The occurrence of the spike is selective in coastal sinkholes (Figure 3).	1. The shape and location of the temperature spikes in the three sinkholes need to be verified by numerical modeling. 2. The upwelling arm of warm sea water further inland has not been located.

sity changes. The halocline shape in Calica Pit is similar to that in Big Calica.

The temperature anomalies in Figure 4, relative to the underlying sea water, are 3.4°C in Big Calica, 1.0°C in Little Calica, and 0.2°C in Calica Pit. Larger anomalies, 3.8° and 1.1°C, respectively, were measured, in profiles taken on different days along the southeast sides of Big Calica and Little Calica. The anomalies in Big and Little Calica are just below the top of the halocline; however, the anomaly in Calica Pit is spread out over the upper halocline.

Temperature anomalies in Figure 4 in Big and Little Calica are larger than those in the historical profiles (Figure 3), because the anomaly peaks over a small depth interval not recorded in the historical profiles. The sea water/ground water temperature below the halocline is 25.5°C in Big Calica, 25.1°C in Little Calica (still within the halocline), and 25.7°C in sea water in the Calica Pit. The trend in the underlying sea water temperature approaching the coast is unclear.

The variation of the temperature anomalies between day and night were examined by hanging the YSI 6600 sonde at a constant elevation, initially corresponding to the depth of the maximum temperature in the halocline, for a 20-hour period in Big Cenote on June 22-23, 2001, and in Little Calica on June 24-25, 2001. To distinguish temperature changes caused by changes in position of the sonde within the halocline as a result of the tide, the range and timing of the daily tidal cycle were determined in Big Calica by hanging an M6015-5PSI-44 probe on a Data Trapper BH1000 water level logger (RST Instruments, Coquittlam, British Columbia, Canada) at constant elevation to measure water-level changes. In Figure 5, the small variations that occurred in temperature corresponded directly to the tidal cycle in which the sonde position in the halocline moved by 2 to 4 cm. The variations were independent of day and night conditions.

Potential Explanations for the Temperature Spikes

The presence and consistency of the temperature spikes in the Calica cenotes throughout the last decade implies that they are unrelated to open-pit mining operations that have occurred in the vicinity during the latter half of the 1990s. Several possible explanations exist for the

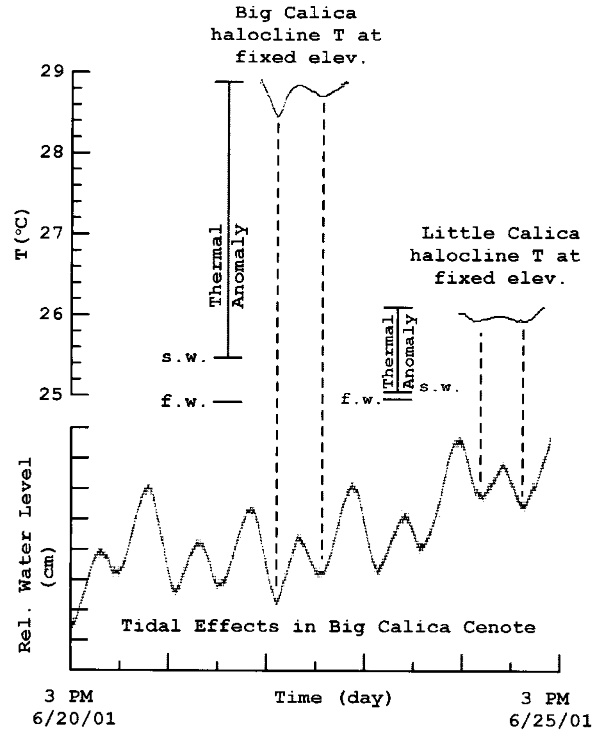

Figure 5. Correlation of tidal effects in Big Calica with temperature fluctuations at a fixed elevation in the halocline in Big Calica and Little Calica.

spikes: in situ absorption of long wavelength light radiation in the halocline; heat generated in situ by exothermic chemical reactions caused by sulfate reduction and/or sulfide oxidation within the halocline and the underlying sea water; or heat generated elsewhere and then transported to the halocline. These explanations are discussed later and listed in Table 1 with observations of consistencies and inconsistencies.

Anomalies Predicted from Radiation Absorption and Chemical Reactions

If in situ absorption of long wavelengths of light radiation is the explanation, a decrease in the temperature should occur at night and the temperature spike should occur in all sinkholes receiving sunlight. The velocity measurements of Soteres (2000) and Moore et al. (1992) imply the halocline fluids can pass through the sinkholes within a half day. Hence, the measured night temperatures in Big Cenote and Little Cenote in Figure 5 were probably not in fluids exposed to light the previous day; therefore, the high heat capacity of water cannot be an explanation for the lack of a decrease in night temperature. Light absorption is also inconsistent with the absence of temperature spikes in Angelita and Chemuyil (Figure 3).

If in situ heat generated by anaerobic chemical reactions is the explanation, the reaction could be sulfate reduction by bacteria (*Desulfovibrio* genus) in the halocline and underlying sea water or oxidation of aqueous sulfide by photosynthetic purple and green bacteria in the halocline. However, this explanation is inconsistent with the lack of a temperature spike in Angelita and Chemuyil (Figure 3) in which these reactions have been documented and the lack of a temperature anomaly in Big Calica below the halocline (Figures 3 and 4) in which sulfate reduction is occurring (Stoessell et al. 1993; Marcella 1994; Stoessell 1992, 1994b). If anaerobic sulfide oxidation by photosynthetic bacteria is the explanation, then the absence of a night decrease in temperature needs to be explained in Big Calica and Little Calica (Figure 5). Another inconsistency results from the lack of anaerobic conditions in Calica Pit. The Eh, measured by the YSI 6600, changed from positive (+100 mv) to negative (−100 mv) just below the top of the halocline in Big Calica and Little Calica, but remained positive in Calica Pit, reflecting the absence of an organic source in the mine area. The observed anomaly in Calica Pit is in aerobic water.

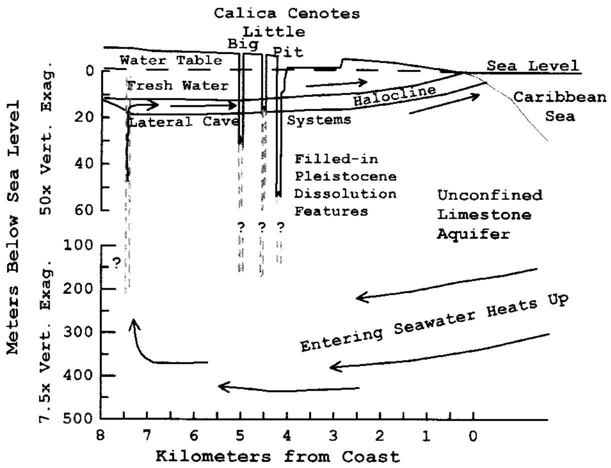

Figure 6. Schematic of the proposed sea water convection cycle in the vicinity of Calica.

If the heat is transported to the halocline, a source and mechanism must be identified. Two possible sources are above and below the halocline. Near the water surface in Figures 3 and 4, the water temperature is affected by the seasonal effect of surface heating; however, the seasonal effect does not extend down to the halocline, tapering off quickly a few meters below the water surface. Because the density of water decreases with rising temperature, heat would have to be transported to the halocline by conduction, a far less effective means than convection. Hence, the heat source was probably below the halocline.

Sea Water Convection as an Explanation for the Anomalies

A localized sea water–convection cell is shown schematically in Figure 6 with the source of heat below the halocline. In this cell, the location of the proposed warm sea water upwelling is landward of the locations of the Calica sinkholes having the temperature anomalies.

Caribbean sea water enters the porous and permeable Pleistocene limestone aquifer along the coast, moves inland through pores and fractures, becoming warmer by heating from the geothermal gradient. When the warm sea water intersects a vertical fracture, buoyancy allows it to rise, displacing cooler sea water. The upward movement is stopped within the halocline by the less-dense but cooler fresh water where it mixes to widen the halocline. Vertical stability occurs within the halocline between two adjacent layers when the overlying layer's temperature is less than 2.5°C cooler per 1 ppt (parts per thousand) decrease in salinity (Fofonoff and Millard 1983), a condition eventually reached because the excess temperature is less than 5°C for the 33 ppt salinity change across the halocline. The warm brackish water flows laterally coastward within the density-stratified halocline, returning to the Caribbean Sea, losing heat to both the overlying fresh water and the underlying sea water.

The upper portion of the vertical fractures in the unconfined Pleistocene limestone aquifer may represent sinkholes and other karst dissolution features that formed when sea level dropped during the Pleistocene Ice Ages. Sea water entering the limestone is supersaturated to calcium carbonate, and dissolution features are expected to form only in the fresh water lens of coastal limestones and in the halocline (Stoessell et al. 1989; Stoessell 1994a). A drop in sea level lowers the position of the halocline, deepening the potential depth of dissolution features.

The depths to the halocline bottom from the present ground surface of some coastal Yucatan sinkholes are sometimes deep, exceeding 30 m in Angelia and Chemuyil and about 40 m in the Calica area. The fact that the halocline sometimes lies above the bottom of the sinkholes is attributed to the rise in sea level since their formation (Stoessell 1994a). Because sea level was as much as 135 m lower during the ice ages, halocline dissolution features could have extended this far below the present halocline. If the climate had higher rainfall, a thicker fresh water lens would have developed, producing halocline dissolution features at even greater depths. Some of these dissolution features may have gradually filled up with limestone debris; however, the features would still provide highly permeable vertical pathways.

Horizontal cave systems in this area would also have formed at greater depths during times of lower sea level, similar to those mapped in the fresh water and shallow saline water by Coke and Young (1989) and Coke et al. (1990) . These deeper caves, even if filled with debris, would provide present-day permeable conduits for sea water in the shallow portion of the sea water convection cell.

The maximum sea water temperature in Big Calica is ~29°C, and the initial temperature of the rising sea water may have been only between 30° and 40°C. Morse and Mackenzie (1990) report that normal to low geothermal gradients for epicontinental carbonate platform deposits on trailing continental margins (such as the Yucatan) are 25° to 30°C per km. The average surface temperature in the Yucatan Peninsula is 25° to 26°C (Back and Hanshaw 1970). Ground water temperatures of 31°C are expected at ground-surface depths of 200 m, the probable vertical extent of Pleistocene dissolution features. A depth of 530 m would be needed for 40°C, implying the flowpath is up fractures because of faulting, rather than dissolution because the associated saline water would be supersaturated to $CaCO_3$.

Comparison of Anomalies with Those Predicted from Sea Water Convection

The selective occurrence of the temperature spikes in coastal sinkholes may be explained by a shallow convection cell localized within the Calica area. The absence of the spikes in the pore system intersected by the Calica boreholes may be caused by selective movement of ground water through the more permeable fracture system connecting the sinkholes, which bypasses much of the pore system represented by the boreholes. The wide halocline in the Calica sinkholes (Figure 4) could be caused by mixing of the rising sea water with the overlying fresh water in vertical fractures upgradient of these sinkholes. The occurrence of the temperature spike within but not below the halocline (Figures 3 and 4) is explained by the Calica sinkholes being along the return arm of the convection cell. Finally, the Calica sinkholes transect (Figure 1) is downgradient in hydraulic head (Moore et al. 1993), making the observed coastward decrease in the magnitude of the temperature spikes consistent with the warm brackish water cooling as it moves coastward.

The shape of the profile of temperature versus depth in the halocline is controlled by cooling into the overlying fresh water and into the underlying sea water. Evidence is lacking for vertical advection across the density-stratified halocline. The analytical solutions of Bredehoeft and Papadopulos (1965), Lu and Ge (1996), and Ge (1998) for modeling the depth-temperature profiles do not apply in fluids that are density stratified.

Dampening of vertical dispersion within the halocline follows from the density stratification (Stoessell 1995). Upward cooling is unlikely to produce a temperature/concentration decrease greater than the 2.5°C/ppt needed for the underlying warm layer to buoyantly rise. Because both the increase in salt concentration and decrease in temperature downward cause density to increase, cooling downward should not alter this trend. The overall stability of the density stratification in the halocline should dampen vertical convection, causing the cooling to be dominated by conduction.

Above the halocline, heat entering the fresh water will cause convection, resulting in a constant temperature boundary at the halocline top, as the warm fresh water rises buoyantly to be replaced by downward sinking cooler fresh water. Hence, conduction cooling upward within the halocline will produce a steep, almost linear, temperature-depth profile connecting the fresh water temperature with the maximum halocline temperature. Beneath this depth of maximum temperature and in the absence of a lower constant-temperature boundary, conductive heat flow downward will create a nonlinear depth-temperature profile. The pattern should be a steep profile ending at the fresh water boundary and a concave profile extending into the underlying brackish sea water. This pattern is shown in the temperature spikes in Figures 3 and 4 in Big Calica and in Figure 4 in Little Calica, but is obscured by the reduced magnitude in the Calica Pit.

Conclusions

A spike exists in the temperature profiles of water depth within the haloclines in three coastal Calica sinkholes aligned along a northwest-southeast 1 km transect towards the Caribbean coast of the Yucatan Peninsula. The magnitude of the spike decreases from 3.5° to 0.2°C in the direction of the coast. One or more of observations concerning the temperature spike—such as its selective occurrence in sinkholes, the temperature spike not occurring in the underlying sea water, and the lack of a change with night conditions—are inconsistent with explanations involving radiation absorption and chemical reactions. However, these observations, together with the general shape of the depth profiles of the temperature spike and the downstream decreasing magnitude trend, are consistent with being on the return arm of a localized shallow sea water convection cell driven by geothermal heating. This hypothesis predicts that warm sea water is rising from depths on the order of 0.5 km in permeable fractures that are further inland than the sinkholes with the temperature spikes. Finding these areas of upwelling would successfully change the hypothesis to a theory.

Acknowledgments

We thank John Clark of Vulcan for access to the Calica sinkholes and Marie Carmen Cerda, Jorge Rodriguez, and Lourdes Rodriguez of CALICA for their assistance. Charles Shaw of Centro Ecologico Akumal provided valuable insight into the geology and hydrology of the Yucatan. Shemin Ge of the University of Colorado and Mary Anderson of the University of Wisconsin, together with two anonymous journal reviewers, made valuable comments that were incorporated into the manuscript. RKS wishes to thank his wife, Londi Moore, for her sacrifice of untold hours of "quality time." The saving grace for her is the beauty of the Caribbean coast.

References

Aharon, P., R.A. Socki, and L. Chan. 1987. Dolomitization of atolls by sea-water convective flow: Test of a hypothesis at Niue, South Pacific. *Journal of Geology* 95, 187–203.

Back, W., and B.B. Hanshaw. 1970. Comparison of chemical hydrogeology of the carbonate peninsulas of Florida and Yucatan. *Journal of Hydrology* 10, 330–368.

Back, W., B.B. Hanshaw, J.S. Herman, and J.N. Van Driel. 1986. Differential dissolution of a Pleistocene reef in the groundwater mixing zone of coastal Yucatan, Mexico. *Geology* 14, no. 2: 137–140.

Beddows, P.A. 1999. Conduit hydrogeology of a tropical coastal carbonate aquifer: Caribbean coast of the Yucatan Peninsula. M.S. thesis, Department of Geography and Geology, McMaster University, Hamilton, Ontario, Canada.

Bredehoeft, J.D., and I.S. Papadopulos. 1965. Rates of vertical groundwater movement estimated from the earths's thermal profile. *Water Resources Research* 1, no. 2: 325–328.

Chen, Y. 1991. Water chemistry of pore fluids in the coastal mixing zone, northeastern Yucatan Peninsula, Mexico. M.S. thesis, Department of Geology and Geophysics, University of New Orleans, Louisiana.

Coke, J.G., and T.M. Young. 1989. Cenote Naharon. An underwater cave map of 4846 m, published by J. Coke and available for purchase at *chac@lcc.net.*

Coke, J.G., J. De Groot, and T.M. Young. 1990. Cenote Carwash. An underwater cave map of 2589 m, published by J. Coke and available for purchase at *chac@lcc.net.*

Cooper, H.H., Jr. 1959. A hypothesis concerning the dynamic balance of freshwater and salt water in a coastal aquifer. *Journal of Geophysical Research* 64, no. 4: 461-467.

Fanning, K.A., R.H. Byrne, J.A. Breland, P.R. Betzer, W.S. Moore, R.J. Elsinger, and T.E. Pyle. 1981. Geothermal springs of the west Florida continental shelf: Evidence for dolomitization and radionuclide enrichment. *Earth Planetary Science Letters* 52, 345–354.

Fofonoff, P., and R.C. Millard Jr. 1983. Algorithms for computation of fundamental properties of seawater. UNESCO *Technical Papers in Marine Sciences* 44.

Ford, B.H. 1985. Geochemistry of water in a coastal mixing zone, northeastern Yucatan Peninsula. M.S. thesis, Department of Geology and Geophysics, University of New Orleans, Louisiana.

Ge, Shemin. 1998. Estimation of groundwater velocity in localized fracture zones from well temperature profiles. *Journal of Volcanology and Geothermal Research* 84, 93–101.

Hanshaw, B.B., and W. Back. 1980. Chemical mass-wasting of the northern Yucatan Peninsula by groundwater dissolution. *Geology* 8, no. 5: 222–224.

Hubbert, M.K. 1940. The theory of ground-water motion. *Journal of Geology* 48, no. 8: 785–944.

Kohout, F.A. 1965. A hypothesis concerning the cyclic flow of salt water related to geothermal heating in the Florida Aquifer. *New York Academy of Science Transactions* 28, no. 2, 249–271.

Kohout, F.A. 1967. Ground water flow and the geothermal regime of the Florida Plateau. *Gulf Coast Association of Geological Sciences Transactions* 17, 339–354.

Lu, N., and S. Ge. 1996. Effect of horizontal heat and fluid flow on the vertical temperature distribution in a semiconfining layer. *Water Resources Research* 32, no. 5: 1449–1453.

Marcella, L.M. 1994. Potential for dolomitization occurring in sea-water salinity fluids in the northeastern Yucatan Peninsula. M.S. thesis, Department of Geology and Geophysics, University of New Orleans, Louisiana.

Moore, Y.H., R.K. Stoessell, and D.H. Easley. 1992. Groundwater flow along the northeastern coast of the Yucatan Peninsula. *Ground Water* 30, no. 3: 343–350.

Moore, Y.H., R.K. Stoessell, and D.H. Easley. 1993. Reply to Discussion of "Groundwater flow along the northeastern coast of the Yucatan Peninsula." *Ground Water* 31, no. 2: 321–322.

Morse, J.W., and F.T. Mackenzie. 1990. *Geochemistry of Sedimentary Carbonates (Developments in Sedimentology,* 48). New York: Elsevier Science.

Saller, A.H. 1984. Petrologic and geochemical constraints on the origin of subsurface dolomite, Enewetak Atoll: An example of dolomitization by normal seawater. *Geology* 12, no. 4: 217–220.

Sanford, W.E., and L.F. Konikow. 1989a. Simulation of calcite dissolution and porosity changes in saltwater mixing zones in coastal aquifers. *Water Resources Research* 25, no. 4: 655–667.

Sanford, W.E., and L.F. Konikow. 1989b. Porosity development in coastal carbonate aquifers. *Geology* 17, no. 3: 249–252.

Simms, M. 1984. Dolomitization by groundwater flow systems in carbonate platforms. *Gulf Coast Association Geological Transactions* 24, 411-420.

Socki, R.A. 1984. A chemical and isotopic study of groundwater from northwestern Yucatan, Mexico. M.S. thesis, Department of Geology, Northern Illinois University, DeKalb, Illinois.

Soteres, A.D. 2000. Groundwater model of freshwater/salt-water lens in the northeastern Yucatan Peninsula. M.S. thesis, Department of Geology and Geophysics, University of New Orleans, Louisiana.

Stoessell, R.K., W.C. Ward, B.H. Ford, and J.D. Schuffert. 1989. Water chemistry and $CaCO_3$ dissolution in the saline portion of an open-flow mixing zone, coastal Yucatan Peninsula, Mexico. *Geological Society America Bulletin* 101, no. 2: 159–169.

Stoessell, R.K., Y.H. Moore, and J.G. Coke. 1993. The occurrence and effect of sulfate reduction and sulfide oxidation on coastal limestone dissolution in Yucatan cenotes. *Ground Water* 31, no. 4: 566–575.

Stoessell, R.K. 1992. Unpublished data from Chemuyil. Available on request.

Stoessell, R.K. 1994a. The effect of past changes in sea level on sulfur redox reactions and karst formation in coastal limestone regions. Karst Waters Institute Inc., *Breakthroughs in Karst Geomicrobiology and Redox Geochemistry*, Colorado Springs, Colorado, Special Publication 1, 69.

Stoessell, R.K. 1994b. Unpublished data from Chemuyil. Available on request.

Stoessell, R.K. 1995. Dampening of transverse dispersion in the halocline in karst limestone in the northeastern Yucatan Peninsula. *Ground Water* 32, no. 3: 366–371.

Swartz, J.H. 1958. Geothermal measurements on Enewetak and Bikini Atolls. U.S. Geological Survey Professional Paper 260-U, 711–739.

Taniguchi, M. 2000. Evaluations of the saltwater-groundwater interface from borehole temperature in a coastal region. *Geophysical Research Letters* 27, no. 5: 713–716.

Ward, W.C., and R.B. Halley. 1985. Dolomitization in a mixing zone of near-seawater composition, Late Pleistocene, northeastern Yucatan Peninsula. *Journal of Sedimentary Petrology* 55, no. 3: 407–420.

Whitaker, F.F., and P.L. Smart. 1990. Active circulation of saline ground waters in carbonate platforms: Evidence from the Great Bahama Bank. *Geology* 18, no. 3, 200–203.